International Journal of GEOMATE, Nov., 2025 Vol.29, Issue 135, pp.180-189
ISSN: 2186-2982 (P), 2186-2990 (O), Japan, DOI: https://doi.org/10.21660/2025.135.5198
Geotechnique, Construction Materials and Environment

EFFECT OF DIFFERENT CRUMB RUBBER SIZES ON IMPROVEMENT OF BUTON ROCK ASPHALT MODIFIED

*Sigit Pranowo Hadiwardoyo[1], Andi Muhammad Ifrad[1], Riana Herlina Lumingkewas[2], Andri Irfan Rifai[3], Dwiky Ihsan Wal Alif[1]

[1]Department of Civil Engineering, Faculty of Engineering, Universitas Indonesia Kampus Baru UI, Depok, Indonesia
[2]Civil Engineering Study Program, Institut Teknologi Indonesia, Kota Tangerang Selatan, Indonesia
[3]Faculty of Civil Engineering and Planning, Universitas Internasional Batam, Indonesia

*Corresponding Author, Received: 26 Aug. 2025, Revised: 23 Sep. 2025, Accepted: 02 Oct. 2025

ABSTRACT: Buton Rock Asphalt contains 20–30% asphalt, and the rest is granular material, so its use is limited due to low penetration value. Mineral granules must be included as aggregates. This study optimizes Buton Rock Asphalt with Waste Engine Oil as a softener and Crumb Rubber from tire waste. Study of Crumb Rubber sizes consists of Large (0.297–0.149 mm), Medium (0.148–0.0075 mm), and Small (<0.0075 mm), each sequentially added to the Buton Rock Asphalt modified. Tests included asphalt physical properties, volumetrics, Marshall properties, viscosity, and modeling using Response Surface Methodology. Crumb Rubber contains the most significant elements of Carbon, 67.57% and oxygen, 21.75%, with small amounts of silicon, potassium, calcium, and copper. The optimum value of Crumb Rubber content based on size is known to be 8% for CR-Large, 5% for CR-Medium, and 1.75% for CR-Small. The lower the Viscosity on Temperature Sensitivity value, the more stable the viscosity to temperature changes, with the following values: CRS (–3.997, CRL (–3.523), and CRM (–3.151). The CRS size type showed the highest Residual Stability Index, meaning it has the resistance to temperature and water changes. Multivariate Polynomial Regression analysis results showed that the addition of CR to BRAM significantly affected the volumetric asphalt concrete mixture. All regression models exhibited a high fit, with R^2 values ranging from 0.95 to 0.98 ($p < 0.0001$). This study is limited to short-term laboratory tests; the performance of Petroleum Asphalt with the involvement of 30% Rock Asphalt still needs further study.

Keywords: Crumb Rubber, Rock Asphalt, Waste Oil, Pavement

1. INTRODUCTION

Rapid population and economic growth have increased traffic loads, coupled with increasingly extreme environmental conditions [1]. As a result, asphalt pavements often experience damage such as ruts, potholes, bumps, and fatigue cracks [2]. These conditions accelerate aging, deformation, cracking, and spalling, which then develop into surface damage in the form of cracks, potholes, and rutting [3-4]. By adding or modifying materials, the physical and chemical properties of asphalt can be improved so that it is more resistant to aging and weather, and has better adhesion and strength [5-6]. Additionally, the incorporation of innovative materials, such as Nano-Expanded Perlite (NEP) and other polymers, has been demonstrated to enhance the softening point, viscosity, and rutting resistance [7].

The use of natural asphalt cannot yet completely replace petroleum asphalt with equivalent mixture proportions. The main drawback is that the material is very granular and brittle, so that excessive use makes the mixture stiffer, more hollow, reduces penetration, increases the softening point, and reduces ductility [8]. Other obstacles include low homogeneity, uneven supply, and difficulty in obtaining good quality. Therefore, optimizing the use of natural asphalt requires improvements in terms of production technology, distribution, and field application. Despite its limitations, this asphalt still provides essential benefits in asphalt mixtures, including increased stability, elasticity, compressive strength, and resistance to deformation. The application of biotechnology to this asphalt mixture has the potential to improve performance and improve its properties [9]. As one improvement solution, modified asphalt is considered important because it can improve pavement performance [10].

As a natural asphalt formed through the polymerization and oxidation of petroleum in the earth's crust of Buton Island, Indonesia, Buton rock asphalt (BRA) has attracted the attention of scientists due to its abundant reserves, high nitrogen content, excellent compatibility with asphalt, and environmental friendliness [11]. BRA can be adopted directly after mining without the need for crude oil refining and can be transported in large quantities at room temperature. BRA has stability at high temperatures so that it can reduce temperature sensitivity. Therefore, it can improve anti-rutting performance. In addition, BRA has a good level of compatibility with petroleum asphalt, so it is easy to mix. The nitrogen content contributes most of the BRA elements, so it easily forms stable compounds with oxygen in the air. Several previous studies also show that the use of BRA requires additional softening agents to reduce stiffness, while increasing resistance to permanent deformation and fatigue cracking [12-13].

The increasing number of vehicles and traffic has increased the amount of engine oil waste. The properties of engine oil degrade with use. Waste Engine Oil (WEO) contains hazardous metals, such as zinc, chlorine, phosphorus, and lead, as well as various other toxic chemicals. Used engine oil poses an ecological problem that can threaten human health, necessitating proper handling of this waste. Petroleum refining produces engine oil and petroleum asphalt. Therefore, WEO has a chemical composition similar to petroleum asphalt (PA). Technically, mixing WEO with PA functions in the regeneration process of old asphalt. Traditional methods of dealing with this waste include disposing of the used engine oil or incineration. Therefore, waste engine oil needs to be reused or recycled as a solution to reduce environmental pollution. Other studies have confirmed that the combination of WEO and BRA produces better rheological properties at both low and high temperature ranges, with a more stable distribution [14]. The properties of natural asphalt are characterized by being wax-free, consisting of large molecules, and being resistant to water and extreme weather [15]. Meanwhile, WEO acts as a softening agent, reducing the stiffness of the asphalt through its asphalt-like molecular properties [16]. Modification with waste materials, such as waste oil and polymers, has been shown to improve durability and reduce costs in mixture modification [17]. This study utilized WEO and used tire rubber fibers in the form of Crumb Rubber (CR). Historically, two main technologies have been used to incorporate Crumb Rubber into hot mix asphalt (HMA) that have been globally accepted for field implementation: (a) the wet process, and (b) the dry process. The use of Crumb Rubber as a modified asphalt material has been widely practiced despite its complex chemical composition, which is influenced by various factors, including rubber components and particle size [18]. The use of CR as an added material in asphalt mixtures effectively reduces environmental pollution. It significantly improves the mechanical properties of asphalt, increasing resistance to rutting deformation, thus extending its service life. Therefore, the integration of WEO is necessary as a softener to overcome the stiffness caused by BRA granular material. The main functional groups in WEO consist of aromatic hydrocarbons, paraffin oils, and polyolefins, which have a molecular structure similar to asphalt [19]. This waste integration aims to improve the physical properties of BRA asphalt mixtures. CR plays a role in increasing deformation resistance in modified asphalt due to its elastic properties, which increases the flexibility of the mixture. Thus, integrating BRA with waste-based modifiers not only improves physical properties but also reduces dependence on petroleum asphalt, contributing to environmental sustainability.

Recent studies have even emphasized the importance of utilizing CR in powder or fiber form to improve the elasticity, wear resistance, and viscoelastic properties of the mixture [20]. The contents of CR and WEO significantly influence the viscoelastic properties and storage stability of the eco-friendly sealant [21-22]. From a methodological perspective, several studies have applied Response Surface Methodology (RSM) with quadratic regression, where parameters serve as response variables to evaluate material performance [23]. This approach demonstrates that analytical method development is as important as material innovation in understanding the behavior of asphalt mixtures.

Based on these reviews, this research focuses on the use of up to 30% natural asphalt (BRA) by integrating WEO waste and CR. The integration of WEO functions as a softener to overcome the stiffness caused by the granular nature of BRA, while CR contributes to increasing the mixture's flexibility through its elastic properties. Based on these considerations, the combination of BRA, WEO, and CR not only enhances the mixture's physical properties but also contributes to reducing the use of petroleum asphalt, providing a sustainable and environmentally friendly solution that optimizes BRA's involvement in the mixture.

2. RESEARCH SIGNIFICANCE

BRA modification using CR and WEO as softening materials directly addresses its stiff and brittle nature, its main weaknesses. Other functions include special characteristics not found in petroleum asphalt, particularly the presence of mineral content inherent in the bitumen. This approach is relevant for producing a mixture that is more flexible, stable, and resistant to tropical conditions. This asphalt has high practical value, especially for road development using local materials that are more flexible and efficient, especially for roads with low to medium traffic loads.

3. RESEARCH METHODS

BRA consists of rock asphalt and fine grains. Its use requires softening material such as WEO. Because the fine grain content is quite high, namely 70-80%. Thus, as a binding material, it still requires additional petroleum asphalt (PA). Optimizing BRA reduces the need for PA.

Experimental studies of the modified asphalt mixture design of BRA with WEO require the CR size to obtain optimal benefits. The sizes are Large (CRL), Medium (CRM), and Small (CRS) fiber CR, for the hot asphalt wearing layer of Asphalt Concrete

Wearing Course (AC-WC) specifications.

CR dimension measurement was performed using a Scanning Electron Microscope (SEM). Identification of BRAM properties is done to optimize the use of PA based on BRAM properties (Fig.1). Furthermore, aggregate requirements are considered by considering the content of fine-grained material in BRA. In contrast, CR is processed into three size fractions. Previous research revealed that CR is added as an asphalt-modifying polymer with a ratio of 3%–8% [22]. However, this study explores a wider range of CR additions (1%–9%) with variations in the sizes of Large, Medium, and Small. The use of BRA is maximized at 30% with the intention of reducing the need for PA to 2%. The use of BRA causes the use of natural aggregates, which is only 70%.

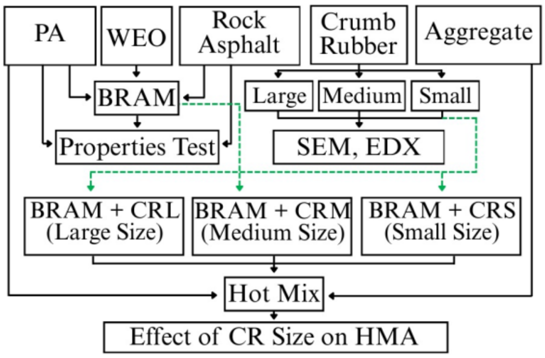

Fig.1 Research Flow

3.1 Materials

3.1.1 Petroleum Asphalt (PA)

This research uses PA with PEN60/70 from PT Pertamina (Persero) in 2022. This type of asphalt is used for road surfaces with varying traffic intensities. The use of BRA in asphalt concrete mixtures still requires PA as a balance for the fine grains in BRA. The characteristics with ASTM Method [24-28] of PEN 60/70 in Table 1.

Table 1. Petroleum Asphalt Pen 60/70 Characteristics

Items	ASTM Method [24-28]	Result	Unit
Penetration	ASTM D-5	68.24	0.1 mm
Softening Point	ASTM-D36	48	°C
Flash Point	ASTM D-92	281.4	°C
Ductility	ASTM-D113	102.7	cm
Specific Gravity	ASTM-D70	1.04	gr/cm^3

3.1.2 Buton Rock Asphalt (BRA)

Rock asphalt in Indonesia comes from Buton Island (Fig.2), Southeast Sulawesi with a rock asphalt (RA) content of 10–40%, with an average of 21.8%. BRA contains fine grain and calcium carbonate ($CaCO_3$). The composition of the mineral content causes low penetration, so that it is stiff and less elastic (Table 2).

Fig.2 BRA mining in Buton Island

Table 2. BRA Bitumen Characteristics

Items	ASTM Method [24-28]	Result	Unit
Penetration	ASTM D-5	26.4	0.1 mm
Softening Point	ASTM-D36	52.34	°C
Flash Point	ASTM D-92	217.00	°C
Ductility	ASTM-D113	50.88	Cm
Specific Gravity	ASTM-D70	1.06	gr/cm^3

3.1.3 Waste Engine Oil (WEO)

WEO is waste oil containing heavy metals that accumulate through physical and chemical processes. Its chemical and physical properties are shown in Table 3 [17].

WEO increased the penetration value of BRA from 26.4 to 95.4, indicating the effectiveness of WEO in softening BRA. WEO 15% resembled PA with a penetration of 66.4 (0.1 mm).

Table 3. Chemical and physical properties of waste engine oil.

Parameter	Value
Chemical Composition	Zn; 749 ppm
	P; 668 ppm
	Ca; 476 ppm
	Mg; 188 ppm
Viscosity (cSt), 60°C	181
Specific gravity (g/cm3)	0.89
Flash point (°C)	193
Loss on heating, % of weight	2.61
Ash content (%)	2.02

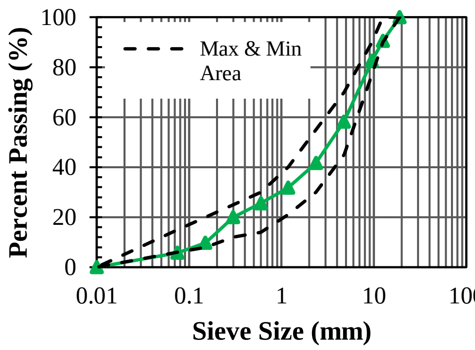

Fig.3 Blending BRA mineral and natural aggregate

3.1.4 Aggregate

The obstacle to maximizing the BRA content in the ACWC asphalt mixture is the high fine-grained material contained in the BRA. The composition of the AC-WC mixture with 30% BRA containing 3.80% fine-grained material is mixed with 70% natural aggregate with 1.34% filler. The combined composition of BRA mineral and natural aggregate is shown in Fig. 3.

3.2 Test and Analysis Program

3.2.1 Extraction of Buton Rock Asphalt (BRA)

The extraction test aims to determine the rock asphalt content in BRA. Therefore, to use BRA as an aggregate binder in asphalt concrete, the amounts of natural aggregate and petroleum asphalt must be determined to calculate the mixture's composition.

The extraction process uses a centrifuge extractor to separate the rock asphalt and mineral fractions from the granular BRA. The mineral fraction is cream-colored, and the bitumen fraction is black (Fig. 4).

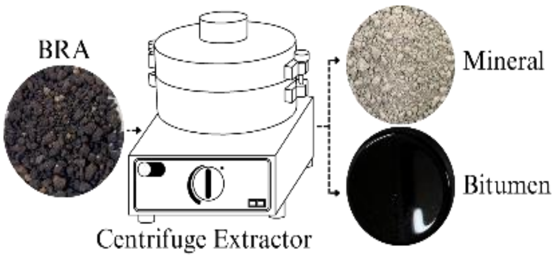

Fig.4 Separation of BRA

3.2.2 Viscosity-Temperature Sensitivity (VTS)

The process of mixing asphalt and aggregate in asphalt concrete is determined by the viscosity value of heated asphalt, which is adjusted to achieve the optimal level of asphalt viscosity for optimal asphalt aggregate adhesion. The determination of Viscosity value is according to ASTM D4402 [28] at a temperature of 135–190°C (cP). Modified BRA samples with the addition of CR in sizes Large (CRL), Medium (CRM), and Small (CRS). Next, to determine the effect of CR dimensions on viscosity values using VTS. And then, to analyze the Temperature sensitivity use the A parameter and VTS value (Eq. 1) [7].

$$\log(\log \eta) = A + VTS \times \log(T_R) \quad (1)$$

Eq. (1) shows the relationship between viscosity and temperature. Where (η) is the asphalt viscosity affected by temperature in degree Rankine (T_R), constant A and VTS as a sensitivity index. High VTS indicates viscosity is highly affected by temperature, while low VTS indicates a more stable viscosity.

3.2.3 Residual Stability Index (RSI)

Asphalt concrete mixes are susceptible to changes in temperature and water. The resistance of asphalt concrete mixes to temperature and water is crucial in determining mix quality, as measured using the Marshall Standard and Marshall Immersion tests. The Marshall test was conducted based on ASTM D5881 standard [30]. Marshall test results are obtained using an Automatic Marshall Stability Test Machine (U-Touch PRO, with a capacity of 50 kN) after the samples are immersed at 60°C for 30 minutes (Marshall Standard) and 24 hours (Marshall Immersion).

The Residual Stability Index (RSI) is used to evaluate the moisture resistance of BRAM, as formulated in Eq. 2.

$$RSI = \frac{\text{MS Immersion}}{\text{MS Standard}} \ (\%) \quad (2)$$

Where MS Immersion is the stability value (kg) with 24-hour immersion, and MS Standard is the stability value (kg) soaked for 30 minutes.

3.2.4 Mini Ball Milling Process

The success of the CR mixing process with asphalt is influenced by the level of distribution in the asphalt. The smaller the CR size, the easier it is to mix. In this study, the CR size consists of three particle sizes CRL, CRM, and CRS using a mini ball milling tool (Fig. 5). The mixing rotation speed is 80 rpm, as well as six steel balls with a diameter of 15 mm and 8 mm. The size of each CR is obtained through variations in milling time with a combination of the same diameter of steel balls rotating in a horizontal direction.

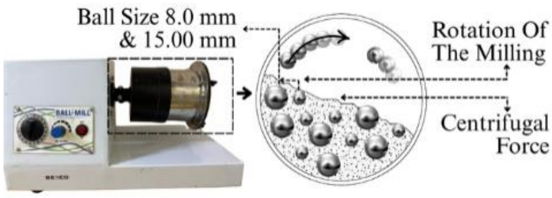

Fig.5 Mini Ball Mill

3.2.5 BRA Modification (BRAM)

The BRA modification process involves softening the BRA using 15% WEO and PA 2%, followed by mixing it with CR to form BRAM-CR. Figure 6 shows the mixing of CR type CRL with a content of (7–10%), CRM (4–7%), and CRS (1–2.5%) into BRAM. This mixture is stored in a closed container for 24 hours to obtain initial homogeneity. BRAM-CR is mixed with aggregate and PA at a temperature of 150°C.

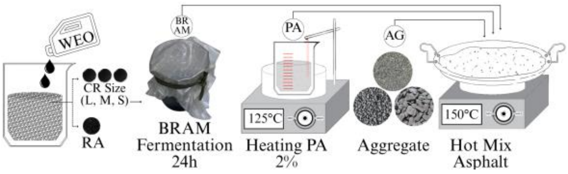

Fig.6 Asphalt Mixture Modification Crumb Rubber

The asphalt concrete mixing process is preceded by heating PA to a temperature of 125 °C and, in parallel, heating the aggregate to a temperature of 150 °C. Next, PA and BRAM-CR are mixed with the aggregate at a mixing temperature of 150 °C (Fig.7).

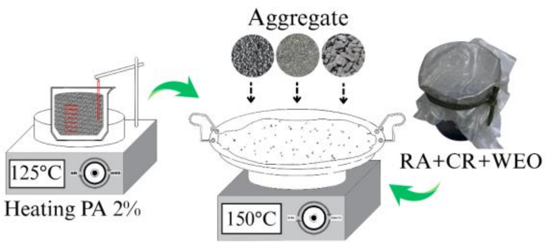

Fig.7 Bitumen Mixture Modification Crumb Rubber

3.2.6 Scanning Electron Microscope (SEM) sample

The use of SEM is intended to determine the size of CR in BRAM. SEM test samples are prepared by mixing BRAM with CR at 100 °C using a stirrer at 2,500 rpm for 60 minutes, as shown in Figure 8.

Fig.8 BRAM-CR process for SEM samples

3.3 Response Surface Methodology (RSM)

RSM evaluates the effect of size and CR content on BRAM characteristics simultaneously. This method is used to determine the interaction between parameters on the mixture response. The design, response modeling, and ANOVA test were performed using OriginLab 2024 (version 10.1). The VIM, VMA, VFA, and density parameters were used as response variables using a quadratic regression approach [23].

4. RESULT

4.1 Identification of Crumb Rubber (CR) Size

The SEM test results (Fig. 9a–c) show each CR size displayed at two different magnifications: 500x and 1,000x. The magnification results show that all types of crumb rubber have an irregular surface and rough texture. From the SEM observation results, it is known that the size of the milled CR fraction is Large (0.297–0.149 mm), Medium (0.148–0.0075 mm), and Small (<0.0075 mm), as in table 5.

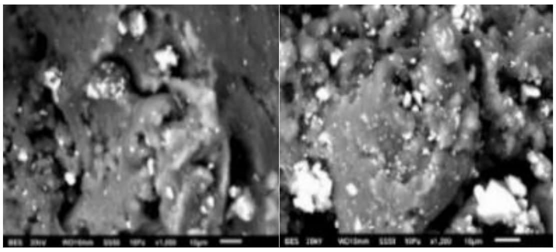

(a) ; Large Size 1000 x (b) ; Medium Size 1000 x

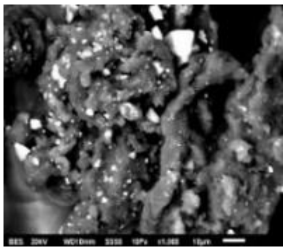

(c) ; Small Size 1000 x

Fig.9 SEM test result

Table 5. Category of Crumb Rubber

Crumb Rubber	Size Range	Unit
Large	0.297–0.149	
Medium	0.148–0.0075	mm
Small	<0.0075	

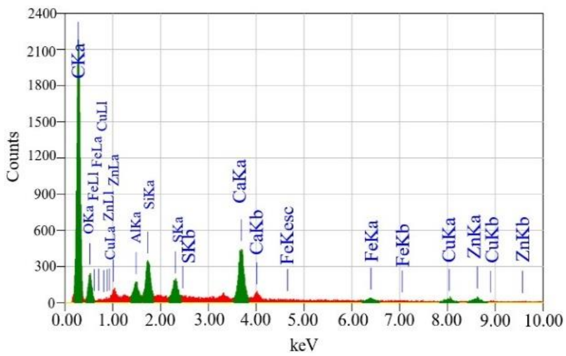

Fig.10 EDX Identification

EDX analysis (Fig. 10) shows the chemical composition of CR. The analysis reveals that it is dominated by carbon (67.57%) and oxygen (21.75%), in the form of organic polymer compounds, such as plastics and resins. Other elements include silicon (7.36%) and potassium (2.89%) in moderate amounts. Calcium (0.18%) and copper (0.13%) are present in small quantities

4.2 Different Size CR on Physical Properties and Viscosity

4.2.1. Physical Properties

In the next stage, samples were selected based on the optimum performance of each sample size, with its respective CR content. The physical properties reviewed are shown in Table 6.

Table 6. Physical Properties BRAM

Sampel	Penetration (0,1 mm) ASTM D-5 [24]	Softening Point (°C) ASTM-D36 [25]	Specific Gravity (g/cm3) ASTM-D70 [28]
PA	68.24	48.00	1.040
BRA	26.40	52.34	1.060
BRAM	68.60	45.80	1.030
CRL 8%	45.80	67.07	1.038
CRM 5%	49.70	64.10	1.034
CRS 1,75%	54.60	69.50	1.040

The test results showed that PA has a penetration of 68.24 (0,1 mm) and a softening point of 48 °C, while BRA is stiffer with a penetration of 26.40 (0.1 mm)and a softening point of 52.34 °C. Modification of BRAM increases the penetration to 68.60 (0.1 mm) and decreases the softening point to 45.80 °C, suitable for light traffic with high flexibility and low temperature crack resistance. The addition of CRL 8% produces a softening point of 67.07 °C and a penetration of 45.80 (0,1 mm), suitable for arterial roads with medium to high temperatures. CRM 5% has a softening point of 64.10 °C and a penetration of 49.70 (0.1 mm), offering a balance between stiffness and flexibility, making it suitable for medium-traffic collector roads. CRS 1.75% with the highest softening point of 69.50 °C and penetration of 54.60 (0,1 mm), suitable for medium to high traffic in hot climates.

4.2.2. Influence of Viscosity on Temperature Sensitivity

Determination of mixing and compaction temperatures to obtain optimal temperatures in the asphalt concrete mixture production process. Viscoelastic property assessment determined a mixing viscosity of 150–190 cP and a compaction viscosity of 250–310 cP [21].

VTS parameters in the viscosity-temperature relationship and to calculate the mixing and compaction temperatures of asphalt binders. All samples had negative VTS values (Fig. 11), PA (–4.194) and CRS (–3.997) showed smaller VTS values, indicating that their viscosity was more stable viscosity under temperature changes. CRS 1.75% (–3.997) had a lower value compared to CRL 8% (–3.523), while BRAM (–2.431), with the higher VTS.

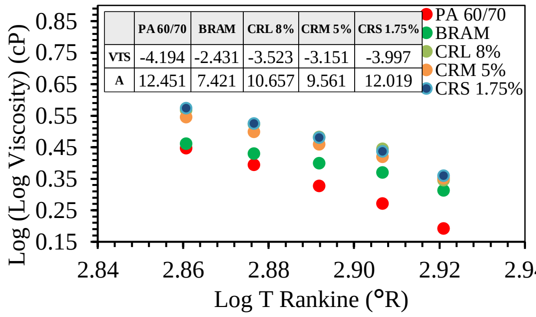

Fig. 11. Viscosity-Temperature Sensitivity

4.3 Susceptibility of BRAM-CR

The susceptibility of BRAM-CR asphalt concrete to temperature and water influences indicates that the size and content of the CR in the asphalt concrete mixture significantly influence the RSI value. Data analysis shows that smaller sizes (CRS) perform better than both CRM and CRL. CRS with a 1-2% content shows the highest RSI value, even higher than BRAM without CR, although its Marshall Stability value is slightly lower (Table 7).

Table 7. Stability BRAM With Different Size CR

CR size-content	Marshall Stability (kg) ±SD %	Marshall Immersion (kg) ±SD %	RSI (%) ±SD %
BRAM	1,085.3 ± 11.7	1000.3 ± 4.8	92.17 ± 17.5
CRS 1%	963.61 ± 5.2	933.21 ± 9.1	96.84 ± 8.5
CRS 1,5%	808.28 ± 30.9	735.54 ± 17.0	91.00 ± 42.5
CRS 2%	800.80 ± 12.4	757.64 ± 23.9	94.61 ± 12.1
CRS 2,5%	794.69 ± 24.3	738.26 ± 35.7	92.90 ± 24.5
CRM 4%	956.82 ± 17.2	897.34 ± 16.4	93.78 ± 27.0
CRM 5%	992.17 ± 18.1	900.74 ± 11.8	90.78 ± 15.5
CRM 6%	872.52 ± 22.2	666.54 ± 28.0	76.39 ± 14.2
CRM 7%	649.21 ± 10.0	543.84 ± 2.9	83.77 ± 7.0
CRL 7%	849.41 ± 3.8	720.59 ± 9.1	84.83 ± 8.5
CRL 8%	825.96 ± 5.8	624.40 ± 35.3	75.60 ± 39.5
CRL 9%	945.60 ± 7.7	491.50 ± 33.9	51.98 ± 42.4
CRL 10%	782.79 ± 20.6	601.28 ± 15.6	76.81 ± 14.6

4.4 Multivariate Polynomial Regression (MPR)

Bazoobandi et al. (2024) [22] used a Multivariate Polynomial Regression (MPR) approach with an i-order polynomial equation (i > 1), where quadratic regression is a special form of a second-order polynomial (i = 2). In this study, a six-parameter model (z_0, a, b, c, d, f) was used to predict VIM, VFA, VMA, and density. This model uses two independent variables: Asphalt Content (AC)% (y), and CR size-content (x), in Eq. 3.

$$Z = z_0 + ax + by + cx^2 + dy^2 + fxy \qquad (3)$$

Eq. (3) builds multivariate relationships through 3D models with Response Surface Methodology. Where Z is the response variable, z_0 is the intercept constant, a and b are the linear coefficients of the *x* and *y* variables, c and d are the quadratic coefficients of x^2 and y^2. f represents the *x–y* interaction. The *x* and *y* variables serve as inputs to the response surface model, as shown in Table 8.

The VIM (Fig. 12a) and VMA (Fig. 12c) models exhibit similar patterns, with Asphalt Content % (y) decreasing linearly and increasing with a positive quadratic effect. CR (x) increases both linearly and quadratically. A negative interaction indicates that the combination of AC and CR content results in a greater decrease in the response.

Table 8. Volumetric BRAM-CR

CR size-content	VIM (%) ±SD %	VMA (%) ±SD %	VFA (%) ±SD %	Density ±SD %
BRAM	3.44 ±22.5	19.44 ±3.3	82.39 ±4.0	2.07 ±0.8
CRS 1%	3.35 ±50.1	19.35 ±7.2	83.01 ±8.6	2.07 ±1.7
CRS 15%	3.36 ±49.9	19.35 ±7.2	82.99 ±8.6	2.07 ±1.7
CRS 2%	3.50 ±25.8	19.46 ±3.8	82.14 ±4.8	2.06 ±0.9
CRS 2,5%	3.44 ±28.8	19.40 ±4.2	82.41 ±5.2	2.07 ±1.0
CRM 4%	3.49 ±18.5	19.42 ±2.7	82.10 ±3.4	2.07 ±0.6
CRM 5%	3.60 ±41.1	19.50 ±6.3	81.80 ±7.6	2.06 ±1.5
CRM 6%	4.15 ±29.9	19.95 ±5.2	79.39 ±6.5	2.05 ±1.3
CRM 7%	4.83 ±15.0	20.50 ±2.9	76.50 ±3.7	2.04 ±0.7
CRL 7%	4.02 ±85.1	19.82 ±14.4	81.0 ±16.6	2.05 ±3.5
CRL 8%	4.49 ±21.2	20.20 ±3.9	77.87 ±4.8	2.04 ±0.9
CRL 9%	4.71 ±45.0	20.38 ±8.7	77.33 ±10.4	2.04 ±2.2
CRL 10%	5.58 ±7.1	21.09 ±1.5	73.55 ±1.9	2.02 ±0.4

The VIM contour moves from 3.3–3.5 at CRS 1–2.5% and CRM 4–5% with AC 8.94–8.95%, to ±4.1–4.8 at CRL 7–9% with AC 8.89–8.91%, and finally to 5.6 at CRL 10% with AC 8.88%. VMA gradients from 19.3–19.7% at CRS 1–2.5% and CRM 4–5% with AC 8.92–8.95%. increased to 21.09% at CRL 10%.

VIM increased with increasing size. CRS had a VIM of around 3.35%, and CRL increased to 5.58%, as did VMA values. Conversely, VFA decreased from 83.01% in CRS to 73.55% in CRL.

The VFA model (Fig. 12. b) is different, where AC% (y) increases to a turning point due to an adverse quadratic effect, while CR (x) decreases linearly and quadratically. A positive interaction indicates a point of balance. The contours show the area of 79.5–83.2% at CRS 1–2.5% and CRM 4% with AC 8.93–8.96%, while the combination of low AC with CRL 7–10% decreases VFA from 81.03%-73.55% at AC 8.88–8.91%.

Table 9. Quadratic Regression Model Parameters

Parameter Model				
$Z = z_0 + a\,x + b\,y + c\,x^2 + d\,y^2 + f\,xy$				
coefficient	VIM	VFA	VMA	Density
z_0	69.39	-247.762	57.932	-1.482
a	58.42	-193.51	48.76	-1.28
b	-15.566	55.564	-12.994	333
c	0.02	-0.04	0.01	0.00
d	873	-3.114	728	-18
f	-6.57	21.71	-5.48	0.14

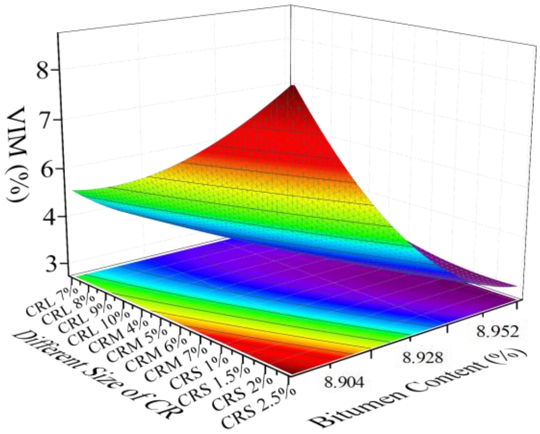

(a) VIM Characteristic

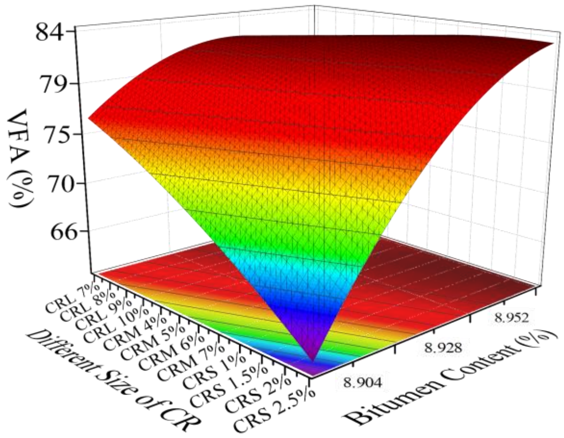

(b) VFA Characteristic

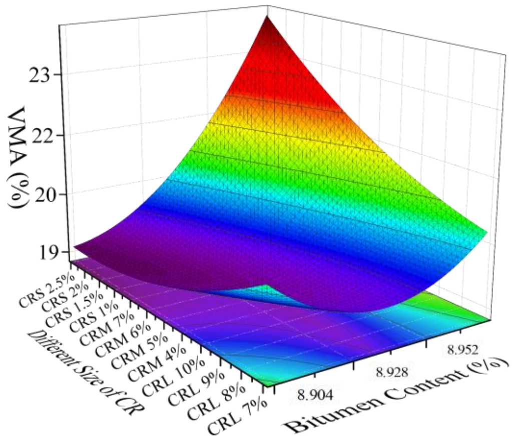

(c)VMA Characteristic

Fig.12 Regression Volumetric Characteristic.

The regression analysis in Table 9 confirms that the larger the CR size, the greater the voids and the interparticle bonding capacity in the mixture. The required AC of each CR size indicates that smaller sizes require more asphalt due to their larger specific surface area and higher adsorption capacity. CRS exhibits the highest density value of 2.07 g/cm³. Small CR sizes produce denser and optimally compacted mixtures.

5. DISCUSSION

SEM results show that CRS (<0.5 mm) has a 25–30% larger surface area than CRL (>1 mm), thus increasing interaction with asphalt. EDX confirms the dominance of carbon (±82%) and oxygen (±12%), that the hydrocarbon properties of recycled tires play a role in adhesion. From a physical perspective, low-percentage CRS (1–2%) showed a PEN of 65–70 and a softening point of 55–58°C, while high-percentage CRL (4–5%) reduced PEN 45–50 with a softening point >62°C, in line with Li et al. (2020) [9] who noted an increase in BRA stiffness after activation treatment.

Observed rheological changes indicate that viscosity increases by approximately 20–35% compared to PA, with the highest viscosity value at 130°C and 1.75% CRS (5.469 cP), followed by 8% CRL (4.819 cP) and 5% CRM (3.144 cP). The increase in viscosity causes an increase in mixing and compaction temperatures of PA from 150°C to 165–170°C (BRAM+CR), and at some point, requires temperatures up to ±189°C to reach working viscosity. This research is in line with the findings of Bazoobandi et al. (2024) [21] that high viscosity values are found in CR-modified binders and additive solutions for mitigation.

Resistance to water and temperature effects, as measured by RSI, showed that CRS had an RSI of 91-97%, while CRL had an RSI of only 52-85%. Suggests that high percentages and large sizes tend to decrease durability due to the formation of excess air voids. This finding is consistent with Wang et al. (2022) [19], who reported that CR tends to degrade over time and weaken binder performance, but this was only similar with larger CR sizes. Lee et al. (2023) [20] reported improvements in fatigue performance with a combination of CR and resin. This study showed that similar improvements were only achieved at the optimal size/percentage on M–CRS 2%, with Marshall stability of 800 kg.

A study based on BRA size showed that BRA was optimized with a combination of WEO and CR. However, this result provides new quantitative evidence that CR particle size is more important than percentage in measuring viscosity, volumetric properties, and RSI. This study was limited to short-term laboratory testing.

Based on Table 10, all regression models for VIM, VFA, VMA, and Density have a very high fit (R^2 = 0.95–0.98) and are statistically significant ($p < 0.0001$). Variables b and d are the main predictors, while a, f, and c have minor effects. VIM and VMA are mainly VFA shows the opposite trend, and Density also follows a curvilinear form under Y.

Table 10. Quadratic Regression of Two Volumetric Variables VIM, VMA, VFA and Density

Regression coefficient					ANOVA					Statistic			
Var.	Coefficient value	Standard error	P Value	Prob>|t|	DF	SS	MS	F Value	Prob>F	RS	RSS	R^2	Adj. R^2
VIM													
z_0	69,391.3	17,894.4	3,878	0,008	5	5.65	1.13	62.19	<0.0001	0.02	0.11	0.98	0.96
a	58.42	24.03	2.431	0.051									
b	-15,566.9	4,029.15	-3.864	0.008									
c	0.02	0.01	1.681	0.144									
d	873.116	226.8	3.850	0.008									
f	-6.56	2.7	-2.425	0.052									
FVA													
z_0	-247,762.7	94,090.5	-2.633	0.039	5	99.98	19.99	39.79	0.00016	0.5	3.01	0.97	0.95
a	-193.5	126.35	-1.532	0.177									
b	55,564.06	21,185.6	2.623	0.039									
c	-0.04	0.05	-0.744	0.485									
d	-3,114.22	1,192.5	-2.611	0.040									
f	21.71	14.23	1.525	0.178									
VMA													
z_0	57,932.2	14,922.7	3.882	0.008	5	3.44	0.69	54.39	<0.0001	0.01	0.08	0.98	0.96
a	48.76	20.04	2.433	0.051									
b	-12,994.5	3,360.03	-3.867	0.008									
c	0.01	0.01	1.682	0.143									
d	728.9	189.14	3.854	0.008									
f	-5.48	2.26	-2.427	0.051									
Density													
z_0	-1482,134	358,511	-4,134	0.006	5	0.002	0.0005	66.07	<0.0001	0.00	0.00	0.98	0.97
a	-1.28	0.48	-2.663	0.037									
b	333.03	80.72	4.126	0.006									
c	0.000	0.000	-1.835	0.116									
d	-18.68	4.54	-4.111	0.006									
f	0.14	0.05	2.656	0.038									

*DF = degree of freedom, SS = Sum of Squares, MS = Mean Square, RS = Reduced Chi-Sqr, RSS = Residual Sum of Squares, R^2 = R-Square (COD)

6. CONCLUSIONS

The main conclusions are as follows:

1. SEM tests revealed the CRL (0.297–0.149 mm), CRM (0.148–0.0075 mm), and CRS (<0.0075 mm) sizes. EDX analysis revealed a dominant carbon content of 67.57% and oxygen of 21.75%, with small amounts of silicon, potassium, calcium, and copper.
2. The effect of CR content on size revealed CRL of 8%, CRM of 5%, and CRS of 1.75%. Based on viscosity values, all samples had negative VTS. The lower the VTS value, the more stable the viscosity is to temperature changes.
3. The addition of CR affected the RSI value of BRAM, with 1% CRS resulting in a value of 96.84% and 9% CRL (51.98%). The RSI value indicates that 1–2% CRS is most effective in increasing BRAM's resistance to temperature and water.
4. Multivariate Polynomial Regression (MPR) results showed that the addition of CR to BRAM significantly affected VIM, VMA, VFA, and density. CRS resulted in higher density, lower VIM, and greater VFA than CRL and CRM. All regression models exhibited a high fit, with R^2 values ranging from 0.95 to 0.98 ($p < 0.0001$).

7. ACKNOWLEDGMENTS

This study was funded by the Faculty of Engineering, Universitas Indonesia (Seed Funding 2024–2025, Contract NKB-3445/UN2.F4.D/PPM . 00.00/ 2024.

8. REFERENCES

1. Chen K., Zhang H., Gu Y., and Zhao S., "Microscopic action and rheological properties of reinforced modified asphalt with varying fiber content," Case Studies in Construction Materials., vol. 18, pp. 1–15, 2023. https://doi.org/10.1016/j.cscm.2023.e01824
2. Goli A., "The study of the feasibility of using recycled steel slag aggregate in hot mix asphalt," Case Studies in Construction Materials., vol. 16, pp. 1–10, 2022 https://doi.org/10.1016/j.cscm.2021.e00861
3. Wang K., Cheng X., Zhu Y., and Li H., "Study on performance deterioration regularity of hot regenerated asphalt mixture under multiple aging factors," Construction and Building Materials., vol. 369, pp. 1–10, 2023. https://doi.org/10.1016/j.conbuildmat.2023.130568
4. Yang X., et al., "Aging behavior of polyphosphoric acid/styrene-butadiene-styrene-modified bio-mixed asphalt based on high-temperature rheological properties and microscopic mechanism," Construction and Building Materials., vol. 389, pp. 1–14, 2023. https://doi.org/10.1016/j.conbuildmat.2023.131691
5. Yang C., et al., "Development of blending model for RAP and virgin asphalt in recycled asphalt mixtures via a micron-Fe3O4 tracer," Journal of Cleaner Production., vol. 383, pp. 1–12, 2023. https://doi.org/10.1016/j.jclepro.2022.135407
6. Han Y., Cui B., Tian J., Ding J., Ni F., and Lu D., "Evaluating the effects of styrene-butadiene rubber (SBR) and polyphosphoric acid (PPA) on asphalt adhesion performance," Construction and Building Materials., vol. 321, pp. 1–12, 2022. https://doi.org/10.1016/j.conbuildmat.2021.126028
.7. Hesami S., Mahzari M., Sobhi S., and Bay M. A., "Investigating the rheological properties and microstructural analysis of Nano-expanded Perlite modified asphalt binder," Case Studies in Construction Materials., vol. 22, pp. 1–20, 2025. https://doi.org/10.1016/j.cscm.2025.e04208
8. Zhang Y., Lu W., Han D., Guo H., Peng X., Zhu W., Xie N., Zuo X., Zhang H., Pan Q., and Xie M., "Laboratory Investigation Of Modified Asphalt Containing Buton Rock Asphalt Or Ash From Buton Rock Asphalt," Case Studies in Construction Materials., vol. 18, pp. 1–21, 2023. https://doi.org/10.1016/j.cscm.2023.e02124
9. Sihombing A. V. R., Subagio B. S., Hariyadi E. S., Mulyadi A. M., Utami R., and Sihombing R. P., "Effect of biorejuvenator types on microstructure, mechanistic performance, and resilient modulus prediction model of asphalt concrete containing recycled materials in Indonesia," Journal of King Saud University - Engineering Sciences. vol. 36, no. 3, pp. 164–174, 2024. https://doi.org/10.1016/j.jksues.2023.04.001
10. Hadiwardoyo S. P., et al., "Improvement of Buton Rock Asphalt Performance by Adding Nano-Crumb Rubber and Waste Engine Oil," International Journal of Pavement Research and Technology., vol. 16, pp. 1181–1195, 2023. https://doi.org/10.1007/s42947-022-00189-4
11. Ren D., et al., "Green and synergistic effects of buton rock asphalt and styrene-butadiene-styrene on asphalt performance: Focus on resistance to thermal oxygen aging," Construction and Building Materials., vol. 453, pp.1-16, 2024. https://doi.org/10.1016/j.conbuildmat.2024.139027
12. Mabui D. S., Tjaronge M. W., Adisasmita S. A., and Pasra M., "Performance Of Porous Asphalt Containing Modificated Buton Asphalt and Plastic Waste," International Journal of

GEOMATE, vol. 18, no. 65, pp. 118–123, 2020, https://doi.org/10.21660/2020.65.67196

13. Gusty S., Israil, Ahmad S. N., and Tumpu M., "Assessing Open-Graded Asphalt'S Resistance To Degradation Via Cantabro Test in Hot-Mix Cold Laid Asbuton," International Journal of GEOMATE, vol. 27, no. 120, pp. 60–68, 2024. https://doi.org/10.21660/2024.120.4488
14. Li Y., Liu Q., Tang J., and Shen Y., "Assessing pavement characteristics: An in-depth evaluation of waste engine oil and Buton rock asphalt composite modified asphalt and its mixture," Construction and Building Materials., vol. 451, no. August, pp. 1–11, 2024. https://doi.org/10.1016/j.conbuildmat.2024.138652
15. Li Y., Guo M., and Liu X., "Macroscopic And Microscopic Characterization Of The Effect Of 'Activation' Process on The Performance Of Buton Rock Asphalt-Modified Asphalt," Advances in Materials Science and Engineering., pp. 1–6, 2020. https://doi.org/10.1155/2020/8148930
16. Liu S., Peng A., Wu J., and Zhou S. B., "Waste engine oil influences on chemical and rheological properties of different asphalt binders," Construction and Building Materials., vol. 191, pp. 1210–1220 2018. https://doi.org/10.1016/j.conbuildmat.2018.10.126
17. Hassan, N. A., Ali, M. F., Rahman, M. A., and Lee, S. H,. "Physical properties of bitumen containing diatomite and waste engine oil," Malaysian Journal of Fundamental and Applied Sciences, 2019. https://doi.org/10.11113/mjfas.v15n4.1230
18. Sun E., Zhao Y., and Wang G., "Nano surface evolution properties of crumb rubber modified asphalt due to aging and adhesion failure mechanism," Construction and Building Materials., vol. 420, February 2024, p. 135564, 2024. https://doi.org/10.1016/j.conbuildmat.2024.135564
19. Wang S., Huang W., Liu, X., and Lin P., "Influence of high content crumb rubber and different preparation methods on properties of asphalt under different aging conditions: Chemical properties, rheological properties, and fatigue performance," Construction and Building Materials., vol. 327, no. November 2021, p. 126937, 2022. https://doi.org/10.1016/j.conbuildmat.2022.126937
20 Lee S. Y., Yun Y. M., and Minh Le T. H., "Influence of performance-graded binders on enhancing asphalt mixture performance with epoxy resin and crumb rubber powder," Case Studies in Construction Materials., vol. 19, no. September, p. e02628, 2023. https://doi.org/10.1016/j.cscm.2023.e02628
21. Bazoobandi P., Mousavi S. R., Karimi F., Karimi H. R., Ghasri M., and Aliha M. R. M., "Cracking resistance of crumb rubber modified green asphalt mixtures, using calcium carbonate nanoparticles and two by-product wax-based warm mix additives," Construction and Building Materials, vol. 424, pp. 1–14, 2024. https://doi.org/10.1016/j.conbuildmat.2024.135848
22. Hu K., Chen Y., Qin M., Hu R., Hu X., and Tao X., "An eco-friendly crack sealant approach for asphalt pavement by using laboratory tests and molecular dynamic simulation," Materials Today Sustainability., vol. 27, no. May, pp. 1–14, 2024. https://doi.org/10.1016/j.mtsust.2024.100893
23. Wei Q., An Y., Zhao X., Li M., Zhang J., and Cui N., "Optimal design of multi-biomaterials mixed extrusion nozzle for 3D bioprinting considering cell activity," Virtual and Physical Prototyping., vol. 20, no. 1, pp. 1–21, 2025. https://doi.org/10.1080/17452759.2024.2438897
.24.ASTM International., "Test Method for Penetration of Bituminous Materials," ASTM International, 1995. https://doi.org/10.1520/D0005_D0005M-20
25. ASTM International., "Test Method for Softening Point of Bitumen (Ring-and-Ball Apparatus)," ASTM International, 2009. https://doi.org/10.1520/D0036_D0036M-09
26. ASTM International., "Test Method for Flash and Fire Points by Cleveland Open Cup Tester," ASTM International, 2005. https://doi.org/10.1520/D0092-24
27. ASTM International., "Test Method for Ductility of Asphalt Materials," ASTM International, 2017. https://doi.org/10.1520/D0113_D0113M-17R23E01
28. ASTM International., "Test Method for Density of Semi-Solid Bituminous Materials (Pycnometer Method)," ASTM International, 1997. https://doi.org/10.1520/D0070-97
29. ASTM International., "Test Method for Viscosity Determination of Asphalt at Elevated Temperatures Using a Rotational Viscometer," ASTM International, 2002. https://doi.org/10.1520/D4402-02
30. ASTM International., "Test Method for Resistance to Plastic Flow of Bituminous Mixtures Using Marshall Apparatus (6 in. Diameter Specimen)," ASTM International, 2007. https://doi.org/10.1520/D5581-25